Journal of Applied Polymer Science

Effect of nucleating agents on the crystallization behavior and heat resistance of poly(L-lactide)

Xiuqin Zhang, Lingyan Meng, Gen Li, Ningning Liang, Jing Zhang, Zhiguo Zhu, Rui Wang
School of Materials Science & Engineering, Beijing Institute of Fashion Technology, Beijing 100029, China
Correspondence to: R. Wang (E-mail: clywangrui@bift.edu.cn)

ABSTRACT: Poly (L-lactide) (PLLA) blends with various nucleators were prepared by melt processing. The effect of different nucleators on the crystallization behavior and heat resistance as well as thermomechanical properties of PLLA was studied systematically by differential scanning calorimetry, X-ray diffraction, heat deflection temperature tester, and dynamic mechanical analysis. It was found that poly(D-lactide), talcum powder (Talc), a multiamide compound (TMC-328, abbreviated as TMC) can significantly improve the crystallization rate and crystallinity of PLLA, thus improving thermal–resistant property. The heat deflection temperature of nucleated PLLA can be as high as 150°C. The storage modulus of nucleated PLLA is higher than that of PLLA at the temperature above T_g of PLLA. Compared with other nucleating agents, TMC was much more efficient at enhancing the crystallization of PLLA and the PLLA containing TMC showed the best heat resistance. © 2015 Wiley Periodicals, Inc. J. Appl. Polym. Sci. **2016**, *133*, 42999.

KEYWORDS: biodegradable; blends; crystallization; properties and characterization

Received 19 June 2015; accepted 4 October 2015
DOI: 10.1002/app.42999

INTRODUCTION

Poly (L-lactide) (PLLA) is a biodegradable polymer produced from plant-derived renewable resources.[1–3] Its good biodegradability, biocompatibility, clarity as well as moderate mechanical properties have made it a suitable choice for many applications.[4–6] It should be noted, however, the poor thermal resistance caused by slow crystallization rate is the main drawback of PLLA in practical applications. The heat deflection temperature (HDT) of PLLA by conventional thermoplastic processing techniques is only about 58°C, which limits the application field of PLLA. The addition of nucleating agent is considered to be the most effective method for improving the crystallization rate and crystallinity of polymers during processing.[7–9] The nucleators can decrease the energy barrier for nucleation and thus initiate the crystallization of polymers at higher temperatures upon cooling. The common nucleating agents mainly include three categories: inorganic, organic, and macromolecular compounds.[9–12]

Talc has been widely used as an inorganic nucleator with low-cost and high-efficiency. The thermo-mechanical properties of nucleated PLLA are improved.[13–16] A multiamide compound (TMC) can also act as highly effective nucleating agent for PLLA.[17,18] Gui *et al.*[18] investigated the effects of eight commercial nucleation agents on the crystallization of PLLA. It was found that TMC-nucleated PLLA possessed the highest crystallization temperature and crystallinity with the same processing condition. The results of Song *et al.* also showed that the crystallization half-time of PLLA decreased sharply with the presence of TMC.[17] Stereocomplex crystals (sc-crystals), formed from the enantiomeric mixture of PLLA and poly(D-lactide) (PDLA),[19–21] can act as a nucleation agent for PLLA crystallization.[22–28] Anderson *et al.*[25] reported that the nucleating efficiency of sc-crystals could reach almost 100% by controlling the appropriate molecular weight and proportion of PDLA. The crystallization half-time of PLLA containing 3 wt % PDLA was less than 1 min at 140°C, which is much lower than 17 min of PLLA and 6.5 min of Talc-nucleated PLLA. However, it was noticed that the crystallinity of PDLA-nucleated PLLA was relatively low compared with that of pure PLLA, which may be attributed to the hindered mobility of PLLA chains bounded to sc-crystals.[27]

Although numerous studies have showed that many nucleating agents could effectively improve the crystallization rate of PLLA,[29–32] there are few reports concerning the effect of nucleating agent on the properties of PLLA under different processing conditions, particularly on heat resistance. In this work, three kinds of typical nucleating agents were selected to tailor the crystallization behavior of PLLA. The relationship between crystallinity and properties was studied systematically. The aim is to provide guidance for preparing the heat-resistant PLLA materials.

EXPERIMENTAL

Materials and Sample Preparation

PLLA (optical purity >99%, M_w = 155 kg/mol, M_n = 96 kg/mol, PDI = 1.62) and PDLA (optical purity >98%, M_w = 135.2 kg/mol,

Table I. The Compositions of Pure and Nucleated PLLA

Sample	PLLA (wt %)	PDLA (wt %)	Talc (wt %)	TMC-328 (wt %)
PLLA	100	-	-	
PLLA-Talc	99.5	-	0.5	
PLLA-TMC	99.5		-	0.5
PLLA-PDLA	95	5		

M_n = 90.0 kg/mol, PDI = 1.50) were kindly provided by Corbion Purac. The particle size of mineral talc is approximately 12 μm (1250 mesh) (LuQuan, HeBei, China). The N,N′,N″-tricyclohexyl-1,3,5-benzene- tricarboxylamide (TMC-328) with a melt temperature of about 375°C was obtained from Shanxi Provincial Institute of Chemical Industry, China. PLLA blends with various nucleators were prepared using a conical twin–screw extruder (Haake PolyLab OS) with a diameter of 16 mm. The temperature profile was 190°C, 200°C, 200°C, and 160°C from hopper to die. The screw speed was set at 80 rpm. Plates for different measurements were prepared using a HAAKE MiniJet with the injection temperature of 200°C. In order to avoid hydrolytic degradation, PLLA, PDLA, Talc, TMC-328 and nucleated PLLA were dried at 80°C under vacuum for 24 hour prior to processing. Sample codes and the content of nucleating agents are shown in Table I.

Measurement and Characterization

The melting and crystallization behavior was carried out on a TA instrument differential scanning calorimetry (DSC) Q2000 under nitrogen atmosphere. The instrument was calibrated with indium before measurements. The samples of about 5–10 mg were weighed and sealed in an aluminum pan, heated to 200°C and held for 5 min to eliminate the thermal history. The samples were first cooled to 50°C at 10°C/min, and then heated to 200°C at 10°C/min.

Wide-angle X-ray Scattering (WAXS) measurements were performed with 5°–35° on Rigaku D/max-2500 (CuKα, λ = 0.154 nm, 40 kV × 200 mA) at room temperature. The crystal size was calculated from the full width at half maximum (FWHM) of the fitted crystalline peaks using the Debye–Scherrer equation expressed as:

$$D_{hkl} = K\lambda/(\beta_{1/2}\cos\theta) \quad (1)$$

Here D_{hkl} represents the mean crystallite size in the normal direction of the (*hkl*) reflection plane and $\beta_{1/2}$ is the FWHM of the diffraction peak (*hkl*) in radians. The shape factor K was set as 0.9 for polymer systems.

According to GB/T1634-2004 method, the heat deflection temperature (HDT) was measured on a HDT/Vicat Tester (JJ-tester, China). The test bars (80 × 10 × 4 mm) were placed to silicon oil as heat transfer medium under the stress of 0.45 MPa. The heating rate was 2°C/min.

Dynamic mechanical analysis (DMA) was performed on a DMA Q800 (TA instrument) in double cantilever beam mode. The dimension of the rectangular specimen was 60 mm × 12 mm × 1.6 mm. The samples were heated from −30°C to 100°C at the rate of 3°C/min. The scan amplitude was set to be 5 μm and the scanning frequency was 1 Hz.

RESULTS AND DISCUSSION

Effect of Nucleators on Crystallization Behavior of PLLA

Figure 1 shows the DSC scans of pure PLLA and its blends. During the cooling process, the crystallization of nucleated PLLA appears at higher temperature compared with pure PLLA, suggesting that Talc, TMC, and PDLA act as effective nucleating agents for PLLA. The crystallization temperatures decrease as follows: PLLA–TMC, PLLA–PDLA, PLLA–Talc, and pure PLLA. It is clearly showed that TMC is much more efficient and PDLA takes the second place.

On the other hand, as is shown in Figure 1(b), a small exothermic peak can be observed prior to the melting of α crystal for pure PLLA. This is attributed to the transformation from α′ to ordered α crystals.[33,34] It was reported that PLLA can crystallize into α form when the crystallization temperature is higher than 120°C and the disordered α′ and ordered α forms can be obtained below 120°C. The absence of the exothermic peak in nucleated PLLA suggests that they mainly crystallize into more stable α form.

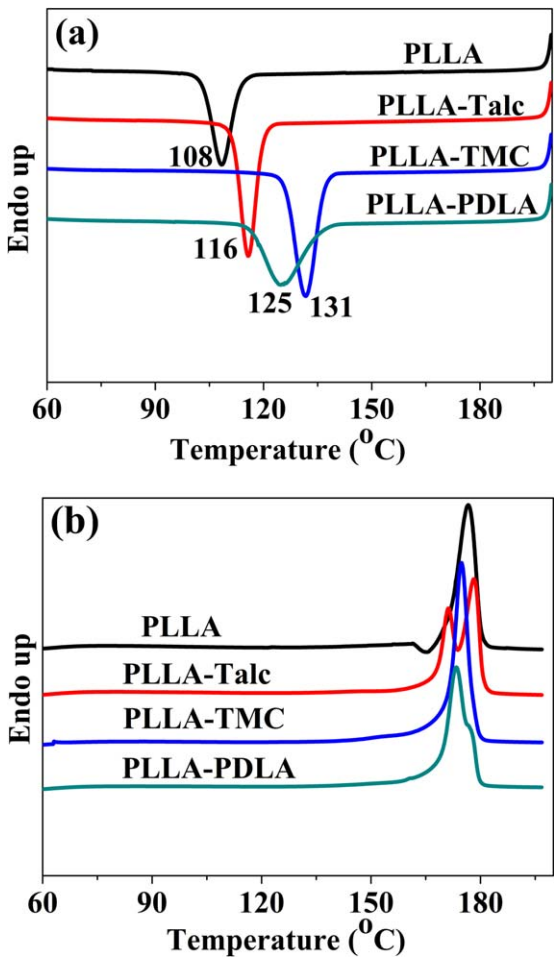

Figure 1. DSC scans of pure and nucleated PLLA: (**a**) cooling curves, (**b**) heating curves. The cooling and heating rates are 10°C/min. [Color figure can be viewed in the online issue, which is available at wileyonlinelibrary.com.]

Table II. Nonisothermal DSC Results for Self-Nucleated PLLA Blends

Nucleator	T_c (°C)	ΔH_c (J/g)	NE (%)
None	113.5	38.7	0
PDLA	133.6	44.2	37.7
Talc	120.9	44.6	13.5
TMC-328	136.6	52.3	42.5

In order to evaluate the nucleating ability of different nucleators, nucleation efficiency (NE) based on the self-nucleation theory was calculated using the following equation[17,25,27,35]

$$\mathrm{NE}=\left(\frac{T_c-T_c^{\min}}{T_c^{\max}-T_c^{\min}}\right)\times 100\% \quad (2)$$

where $T_c^{\max}$ and $T_c^{\min}$ for the homopolymer were measured according to a self-nucleation experiment as described in the literature.[27] $T_c^{\max}$ was the maximum crystallization temperature from a "self-nucleated" melt in which the stable nuclei reach saturation. $T_c^{\min}$ was the lowest crystallization temperature from the melting with minimum nuclei. The test procedures of $T_c^{\max}$ and $T_c^{\min}$ of PLLA were employed as follows: (i) PLLA was heated to 200°C at 20°C/min and held for 5 min to erase the thermal history. Then, PLLA was cooled to 80°C from 200°C at 5°C/min, and the observed crystallization peak (T_c) is equal to $T_c^{\min}$ in the absence of pre-existing nuclei. (ii) According to the melting curve of PLLA, the partial melting zone (175°C–180°C) was decided.[27] PLLA was heated to the lower limit of the partial melting zone (175°C) and held for 5 min to create saturated self-nucleated sites. $T_c^{\max}$ was obtained after cooling from 175°C to 80°C at 5°C/min. $T_c^{\max}$ and $T_c^{\min}$ were measured to be 168.0°C and 113.5°C, respectively. T_c of nucleated PLLA was determined by quickly heating the samples to 200°C (20°C above the predetermined PLLA "melt-out" temperature). At the 200°C, the α crystals were completely melted, but the nucleators (Talc, TMC, and sc-crystals) were left. After holding 5 min at 200°C, the samples were cooled and the T_c and the area of crystallization exotherm (ΔH_c) were recorded. The NE values were then calculated using eq. (2), as shown in Table II.

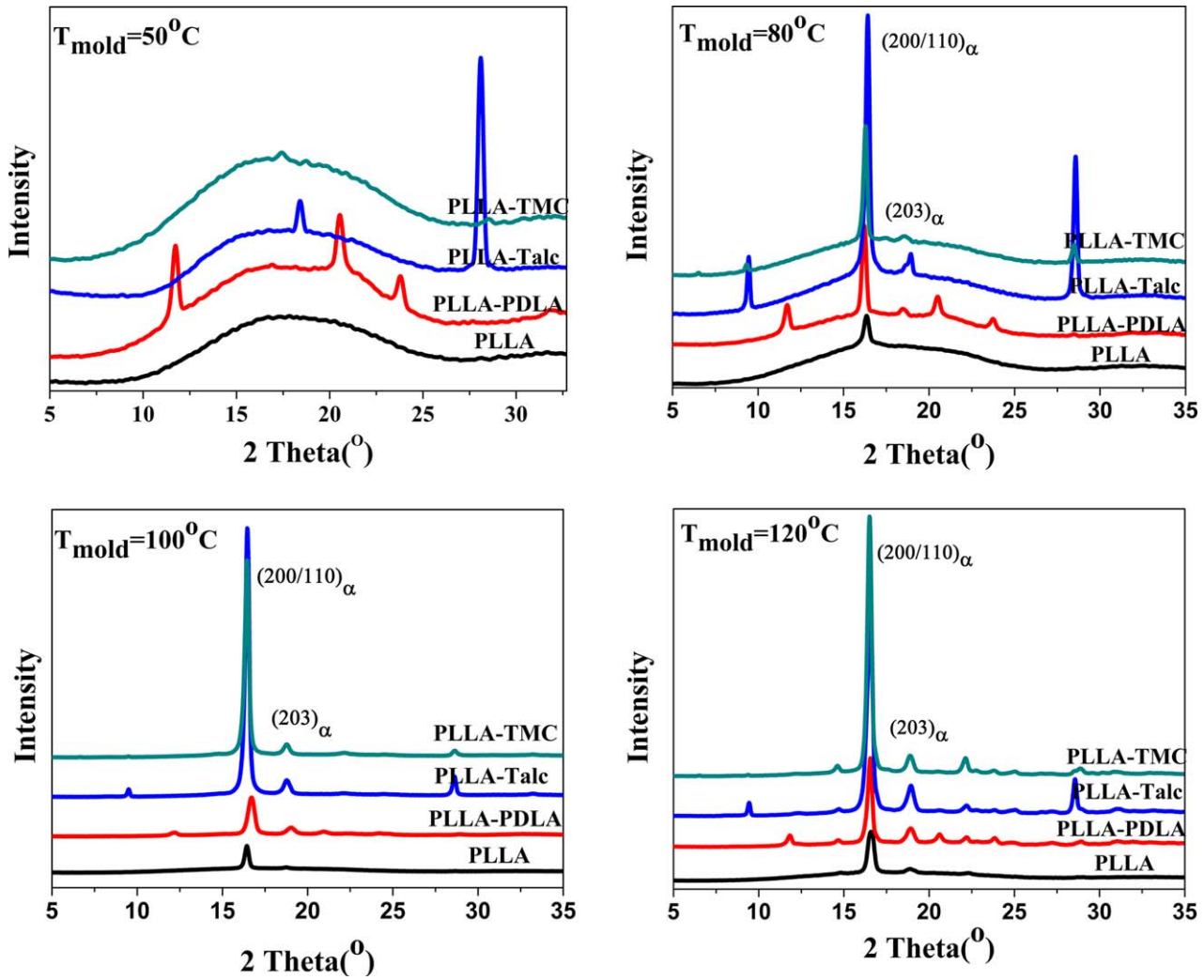

Figure 2. WAXS intensity curves of PLLA and nucleated PLLA prepared at various mold temperatures. [Color figure can be viewed in the online issue, which is available at wileyonlinelibrary.com.]

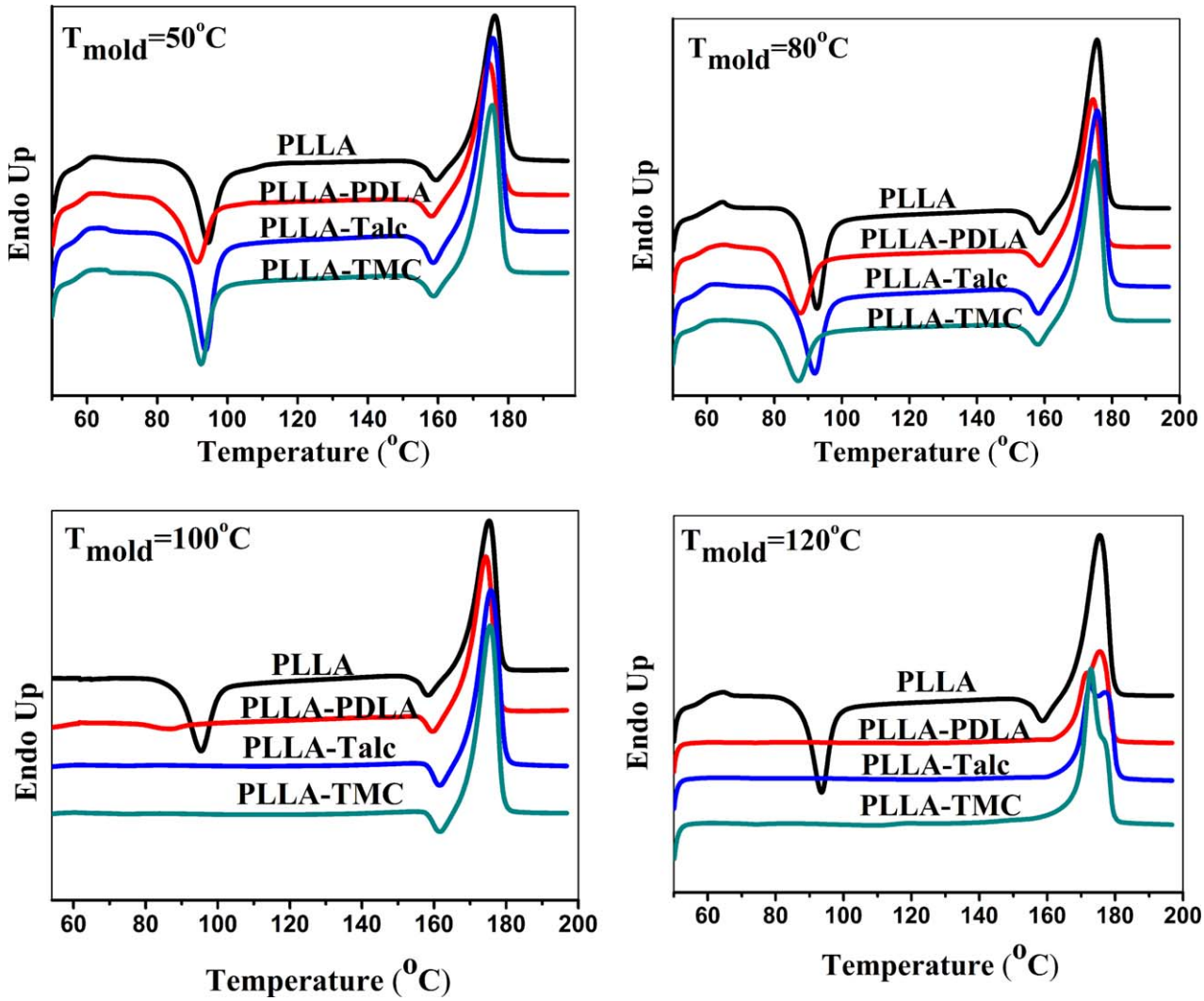

Figure 3. DSC heating curves of PLLA and nucleated PLLA prepared at various mold temperatures. [Color figure can be viewed in the online issue, which is available at wileyonlinelibrary.com.]

The results showed that TMC-328 shows the highest nucleation efficiency and results in the highest crystallinity of PLLA. PDLA (sc-crystals) was a superior nucleating agent compared with Talc. The NE of PDLA is 37.7%, which is nearly three times compared with that of Talc with 13.5%. However, the crystallization enthalpy of PLLA blends with Talc or PDLA was almost equal. As reported previously,[36,37] the network of sc-crystals formed by PLLA and PDLA confined the mobility of PLLA chain segments, thus decreasing the crystal growth rate, which influenced the crystallinity of PLLA. Another possible reason is that part of the PLLA cannot participate in α crystal, as it has been co-crystallized with PDLA as sc-crystals.

Crystallization Behavior of Injection-Molded Plates

To prepare samples with different crystallinity, the mold temperatures (T_{mold}) were selected from 50°C to 120°C and the annealing time was 1 min. The WAXS curves of PLLA and nucleated PLLA plates prepared at different mold temperatures were shown in Figure 2.

When molded at 50°C, PLLA displayed a diffuse halo, suggesting that it is amorphous. Three diffraction peaks at $2\theta = 11.8°$, 20.7°, and 23.9° were observed in PDLA-nucleated PLLA, which are assigned to the (110), (300/030), and (220) planes of sc-crystals, respectively.[20,38,39] The diffraction peaks for Talc in PLLA-Talc at $2\theta = 9.5°$, 18.4°, and 28.1° can be observed.[40] No α crystal could be seen in all injection-molded plates when the mold temperature was set at 50°C.

When the mold temperature is 80°C, there are two diffraction peaks for the PLLA and nucleated PLLA plates at $2\theta = 16.3°$ and 18.9°, which can be assigned to the crystal planes (200)/(110) and (203) of α or α′ crystal forms of PLLA, respectively.[39,41–44] When the mold temperature further increases, the diffraction intensities of crystalline peaks become stronger, suggesting the increase of crystallinity in injection-molded plates, especially for PLLA-Talc and PLLA-TMC plates. The mean crystallite size (D) in the direction perpendicular to crystal planes (203) can be estimated using the width of the peak at half-maximum by Debye–Scherrer formula. The crystallite size of pure PLLA is approximately 12.9 nm, while the PLLA blends

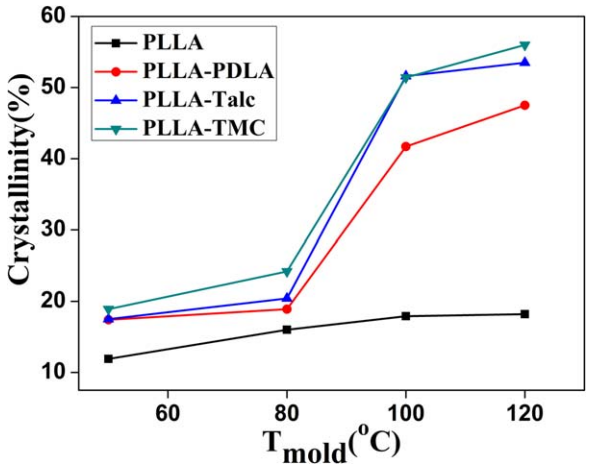

Figure 4. Crystallinity of PLLA and nucleated PLLA plates prepared at different mold temperatures. [Color figure can be viewed in the online issue, which is available at wileyonlinelibrary.com.]

with TMC or PDLA or Talc is approximately 18.4 nm, approximately 19.0 nm, approximately 19.1 nm, respectively. It reveals that the crystal structure of nucleated PLLA plates prepared at 120°C is more perfect than that of pure PLLA.

Figure 3 shows the DSC heating curves of injection-molded PLLA plates. An exothermic cold crystallization peak at approximately 90°C and a transition peak from α′ to α crystals were observed in the PLLA and nucleated PLLA plates prepared at 50°C or 80°C, suggesting that the initial crystallinity formed during injection-molded processing was low. When the mold temperature was 100°C or 120°C, for pure PLLA plate, the exothermic cold crystallization peak was still visible, while the cold crystallization peaks disappear for nucleated PLLA plates, suggesting that the nucleated PLLA fully crystallized under this condition during processing. Furthermore, there is no transition peak from α′ to α crystals for nucleated PLLA plates prepared at 120°C mold temperature, revealing that the ordered α form was formed at this processing condition. The results are consistent with the WAXS data. The crystallinity can be calculated using the following formula.

$$X_c = \frac{\Delta H_m - \Delta H_{cc}}{\Delta H_m^o} \quad (3)$$

where ΔH_m is the melting endothermic enthalpy and ΔH_{cc} is the cold crystallization enthalpy during DSC heating scan. ΔH_m^o is the melting enthalpy of α crystal of PLLA with 100% crystallinity (93 J/g).[19] The results are shown in Figure 4. It is found that the crystallinity of nucleated PLLA is slightly higher than that of pure PLLA plates when the mold temperature is 50°C or 80°C. With the increase of mold temperature (100°C or 120°C), the crystallinity of nucleated PLLA significantly increases, far above the pure PLLA plates prepared at the same injection-molded condition. Especially, PLLA containing TMC or Talc shows the highest crystallinity. It is noteworthy that there is no diffraction peak of α or α′ crystals in WAXS curves of PLLA and nucleated PLLA plates prepared at 50°C (Figure 2), while the crystallinity of plates from DSC data exceeds 10%. This discrepancy might be due to the potential crystallization during the heating.[45] The crystallinity estimated from WAXS data relies on a deconvolution of the WAXS intensity profiles into an amorphous halo and the sum of the crystalline components, which leads to some error. Furthermore, according to the WAXS curves (Figure 2) and DSC profiles (Figure 3), the trends of variation of crystallinity with the mold temperatures are similar. Therefore, only crystallinity from DSC data is presented.

Heat Resistance Analysis of Injection-Molded Plates

Polymer's crystallinity plays a significant role in the material's heat resistance. For the amorphous polymers or polymers with low crystallinity, the heat resistance is determined by the glass transition temperature (T_g), while the heat resistance of polymers with high crystallinity depends on the melting temperature of crystals. Figure 5 shows the dependence of HDT on the mold temperature. The HDT of PLLA and nucleated PLLA plates prepared at 50°C or 80°C is low and near T_g of PLLA due to the low crystallinity. For nucleated PLLA prepared at 100°C and 120°C, the HDT is above 100°C due to the high crystallinity, while HDT of pure PLLA is still low at the same condition. In addition, the HDT of TMC-nucleated PLLA reaches to 150°C

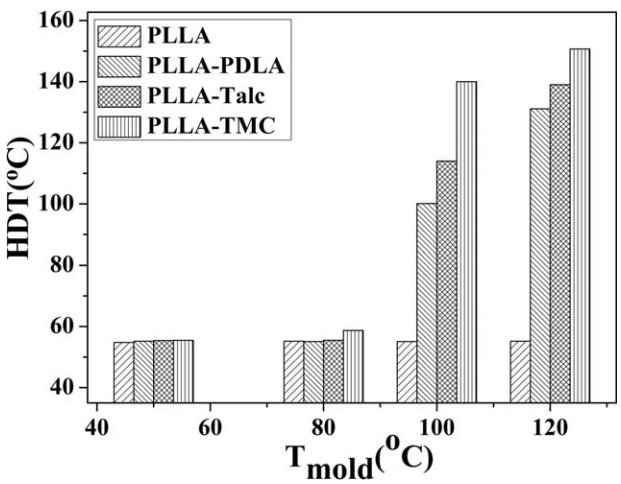

Figure 5. HDT of injection-molded plates prepared at different mold temperatures.

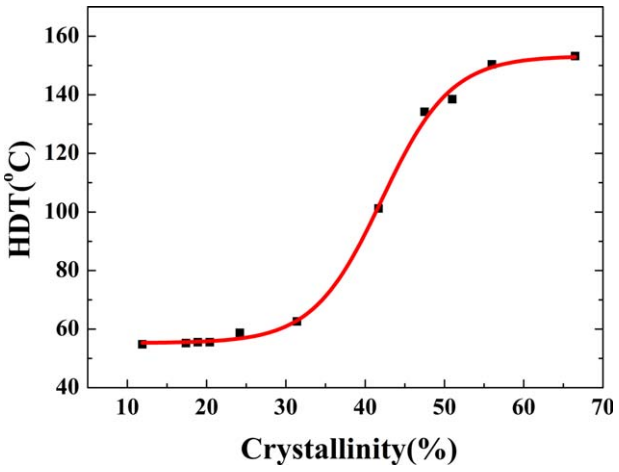

Figure 6. HDT of injection-molded plates as a function of crystallinity. [Color figure can be viewed in the online issue, which is available at wileyonlinelibrary.com.]

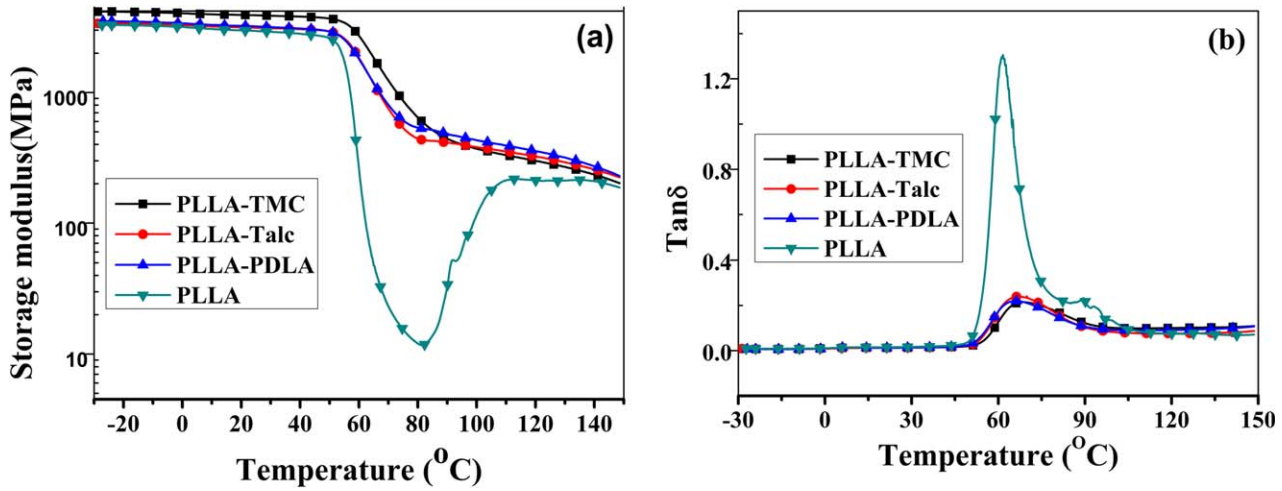

Figure 7. (a) Storage modulus and (**b**) tanδ versus temperature curves of the injection-molded PLLA and nucleated PLLA prepared at mold temperature of 120°C. [Color figure can be viewed in the online issue, which is available at wileyonlinelibrary.com.]

due to the high crystallinity of 55%. The improvement on heat resistance of PLLA may broaden the application and promote the development of PLLA with high performance.

In order to further determine the relationship between crystallinity and HDT, samples with different crystallinity (0%–66%) were prepared by controlling the conditions of injection molding. The crystallinities of samples were measured by DSC at a heating rate of 10°C/min. An S-shaped curve was observed in Figure 6. A low HDT level around T_g is found when the crystallinity is below 30%, while the significant increase of HDT happens when the crystallinity exceeds 30%. Further increasing the crystallinity to 55%, there is no dependence of the HDT on the crystallinity, and the biggest HDT is about 155°C, which is near the onset melting temperature of α crystals. The correlation between crystallinity and HDT may provide a theoretical reference for developing heat resistant PLLA materials.

Thermomechanical Properties

To explore the importance of improving the crystallinity of PLLA in practical applications, the injection-molded PLLA and nucleated PLLA plates prepared at molding temperature of 120°C were analyzed with DMA. The dynamic mechanical behavior of PLLA and nucleated PLLA from −30°C to 150°C was investigated. Figure 7 presents the variation of the storage modulus (E') and tanδ as a function of temperature. In the low temperature zone (lower than T_g of PLLA), pure PLLA exhibits the storage modulus of 3301 MPa, while PLLA with TMC, PDLA, or Talc have the modulus of 4160, 3502, and 3386 MPa, respectively [Figure 7(a)]. The difference is relatively low. With increasing the temperature to 50°C near the Tg of PLLA, the modulus of pure PLLA shows a sharp fall between 50°C and 80°C. The modulus of nucleated PLLA also decreases, while it can remain the level of about 500 MPa with the increase of temperature. It is noteworthy that the modulus of PLLA increases again when the temperature is above 80°C. Combining with the date of DSC (Figure 3, $T_{mold} = 120$°C), the onset temperature of cold crystallization of PLLA during the heating is about 80°C, indicating the increase of modulus of PLLA is related with the crystallization of PLLA during heating. In addition, as is shown in Figure 7(b), the glass transition temperature increases slightly from 61.8°C for pure PLLA to 67°C for nucleated PLLA. Due to the high crystallinity of nucleated PLLA, the chain motion was depressed at the T_g, resulting in a significant decrease of the area underneath the tanδ peak.

CONCLUSIONS

The present work reported the crystallization behavior and heat resistance of PLLA and nucleated PLLA under different processing conditions. Moreover, the correlation between crystallinity and HDT was founded, which provided guidance for developing heat resistant PLLA materials. The nucleating agent showed a significant promoting effect on the crystallization rate and crystallinity of PLLA, in particular, TMC showed the highest nucleation efficiency at the same condition. When injection molded at higher temperature, the nucleated PLLA exhibited a much higher HDT. The HDT of TMC-nucleated PLLA reached as high as 150°C. More importantly, the injection-molded PLLA with nucleator showed the relatively high thermal mechanical property at the temperature higher than T_g of PLLA. This work could provide guidance toward industrial-scale fabrication of PLA products with high heat resistance using conventional melt-processing equipment.

ACKNOWLEDGMENTS

The work was financially supported by Program for New Century Excellent Talents in University (NCET-12-0601) and Beijing Training Project for the Leading Talents in S & T (LJ201305) and Beijing Municipal Natural Science Foundation (KZ201310012014). The authors thank Corbion Purac Company for kindly providing the PLA samples.

REFERENCES

1. Sodergard, A.; Stolt, M. *Prog. Polym. Sci.* **2002**, *27*, 1123.
2. Drumright, R. E.; Gruber, P. R.; Henton, D. E. *Adv. Mater.* **2000**, *12*, 1841.

3. Vaidya, A. N.; Pandey, R. A.; Mudliar, S.; Kumar, M. S.; Chakrabarti, T.; Devotta, S. *Crit. Rev. Env. Sci. Technol.* **2005**, *35*, 429.
4. Gupta, B.; Revagade, N.; Hilborn, J. *Prog. Polym. Sci.* **2007**, *32*, 455.
5. Auras, R.; Harte, B.; Selke, S. *Macromol. Biosci.* **2004**, *4*, 835.
6. Madhavan, N. K.; Nair, N. R.; John, R. P. *Bioresour. Technol.* **2010**, *101*, 8493.
7. Liu, G. M.; Zhang, X. Q.; Wang, D. J. *Adv. Mater.* **2014**, *26*, 6905.
8. Xing, Q.; Zhang, X. Q.; Dong, X.; Liu, G. M.; Wang, D. J. *Polymer* **2012**, *53*, 2306.
9. Saeidlou, S.; Huneault, M. A.; Li, H.; Park, C. B. *Prog. Polym. Sci.* **2012**, *37*, 1657.
10. Tsuji, H.; Takai, H.; Fukuda, N.; Takikawa, H. *Macromol. Mater. Eng.* **2006**, *291*, 325.
11. Zhao, H. W.; Bian, Y. J.; Li, Y.; Han, C. Y.; Dong, Q. L.; Dong, L. S.; Gao, Y. *Thermochim. Acta* **2014**, *588*, 47.
12. Bai, H.; Huang, C.; Xiu, H.; Zhang, Q.; Fu, Q. *Polymer* **2014**, *55*, 6924.
13. Li, H. B.; Huneault, M. A. *Polymer* **2007**, *48*, 6855.
14. Ke, T.; Sun, X. *J. Appl. Polym. Sci.* **2003**, *89*, 1203.
15. Penco, M.; Spagnoli, G.; Peroni, I.; Rahman, M. A.; Frediani, M.; Oberhauser, W.; Lazzeri, A. *J. Appl. Polym. Sci.* **2011**, *122*, 3528.
16. Battegazzore, D.; Bocchini, S.; Frache, A. *Express. Polym. Lett.* **2011**, *5*, 849.
17. Song, P.; Wei, Z. Y.; Liang, J. C.; Chen, G. Y.; Zhang, W. X. *Polym. Eng. Sci.* **2012**, *52*, 1058.
18. Gui, Z.; Lu, C.; Cheng, S. *Polym. Test.* **2013**, *32*, 15.
19. Tsuji, H. *Macromol. Biosci.* **2005**, *5*, 569.
20. Ikada, Y.; Jamshidi, K.; Tsuji, H.; Hyon, S. H. *Macromolecules* **1987**, *20*, 904.
21. Okihara, T.; Tsuji, M.; Kawaguchi, A.; Katayama, K.; Tsuji, H.; Hyon, S. H.; Ikada, Y. *J. Macromol. Sci. Phys.* **1991**, *B30*, 119.
22. Wei, X. F.; Bao, R. Y.; Cao, Z. Q.; Yang, W.; Xie, B. H.; Yang, M. B. *Macromolecules* **2014**, *47*, 1439.
23. Narita, J.; Katagiri, M.; Tsuji, H. *Macromol. Mater. Eng.* **2011**, *296*, 887.
24. Tsuji, H.; Takai, H.; Saha, S. K. *Polymer* **2006**, *47*, 5430.
25. Anderson, K. S.; Hillmyer, M. A. *Polymer* **2006**, *47*, 2030.
26. Yamane, H.; Sasai, K. *Polymer* **2003**, *44*, 2569.
27. Schmidt, S. C.; Hillmyer, M. A. *J. Polym. Sci., Part B: Polym. Phys.* **2001**, *39*, 300.
28. Wei, X. F.; Bao, R. Y.; Gu, L.; Wang, Y.; Ke, K.; Yang, W.; Xie, B. H.; Yang, M. B.; Zhou, T.; Zhang, A. M. *Rsc Adv.* **2014**, *4*, 2733.
29. Fan, Y. Q.; Yu, Z. Y.; Cai, Y. H.; Hu, D. D.; Yan, S. F.; Chen, X. S.; Yin, J. B. *Polym. Int.* **2013**, *62*, 647.
30. Xing, Q.; Li, R. B.; Dong, X.; Luo, F. L.; Kuang, X.; Wang, D. J.; Zhang, L. Y. *Macromol. Chem. Phys.* **2015**, *216*, 1134.
31. Xu, T.; Wang, Y. M.; Han, Q.; He, D. R.; Li, Q.; Shen, C. Y. *J. Macromol. Sci. Part B-Phys.* **2014**, *53*, 1680.
32. Xu, T.; Zhang, A. J.; Zhao, Y. Q.; Han, Z.; Xue, L. X. *Polym. Test.* **2015**, *45*, 101.
33. Kawai, T.; Rahman, N.; Matsuba, G.; Nishida, K.; Kanaya, T.; Nakano, M.; Okamoto, H.; Kawada, J.; Usuki, A.; Honma, N.; Nakajima, K.; Matsuda, M. *Macromolecules* **2007**, *40*, 9463.
34. Sarasua, J. R.; Arraiza, A. L.; Balerdi, P.; Maiza, I. *J. Mater. Sci.* **2005**, *40*, 1855.
35. Xu, Y.; Wang, Y.; Xu, T.; Zhang, J.; Liu, C.; Shen, C. *Polym. Test.* **2014**, *37*, 179.
36. Yin, Y. A.; Zhang, X. Q.; Song, Y.; De Vos, S.; Wang, R. Y.; Joziasse, C. A. P.; Liu, G. M.; Wang, D. J. *Polymer* **2015**, *65*, 223.
37. Rahman, N.; Kawai, T.; Matsuba, G.; Nishida, K.; Kanaya, T.; Watanabe, H.; Okamoto, H.; Kato, M.; Usuki, A.; Matsuda, M.; Nakajima, K.; Honma, N. *Macromolecules* **2009**, *42*, 4739.
38. Xiong, Z. J.; Liu, G. M.; Zhang, X. Q.; Wen, T.; de Vos, S.; Joziasse, C.; Wang, D. J. *Polymer* **2013**, *54*, 964.
39. Zhang, X.; Xiong, Z.; Liu, G. Y. A.,Y.; Wang, R.; Wang, D. *Acta Polym. Sin.* **2014**, *8*, 1048.
40. Suh, C. H.; White, J. L. *J. Non-Newton. Fluid Mech.* **1996**, *62*, 175.
41. Zhang, X.; Schneider, K.; Liu, G.; Chen, J.; Brüning, K.; Wang, D.; Stamm, M. *Polymer* **2012**, *53*, 648.
42. Zhang, X.; Schneider, K.; Liu, G.; Chen, J.; Brüning, K.; Wang, D.; Stamm, M. *Polymer* **2011**, *52*, 4141.
43. Zhang, J.; Tashiro, K.; Tsuji, H.; Domb, A. J. *Macromolecules* **2008**, *41*, 1352.
44. Xiong, Z.; Zhang, X.; Liu, G.; Zhao, Y.; Wang, R.; Wang, D. *Chem. J. Chin. Univ.* **2013**, *34*, 1288.
45. Srithep, Y.; Nealey, P.; Turng, L. S. *Polym. Mater. Sci. Eng.* **2013**, *53*, 580.